AGU PUBLICATIONS

Geophysical Research Letters

RESEARCH LETTER

10.1002/2014GL059408

Key Points:

- The Vp/Vs ratios decrease substantially in the precursory and explosive phases
- High Vp/Vs ratios are observed over a wide region before explosive eruptions
- Decrease of gas and melts by about 1.1 and 7.9 GPa before and during eruptions

Supporting Information:

- Readme
- Table S1 and Figures S1–S7

Correspondence to:
T.-K. Hong,
tkhong@yonsei.ac.kr

Citation:
Hong, T.-K., S. E. Houng, and E. Jo (2014), Temporal changes of medium properties during explosive volcanic eruption, *Geophys. Res. Lett.*, *41*, 1944–1950, doi:10.1002/2014GL059408.

Received 24 JAN 2014
Accepted 6 MAR 2014
Accepted article online 11 MAR 2014
Published online 24 MAR 2014

Temporal changes of medium properties during explosive volcanic eruption

Tae-Kyung Hong[1], Soung Eil Houng[1], and Eunyoung Jo[1,2]

[1]Department of Earth System Sciences, Yonsei University, Seoul, South Korea, [2]Now at National Institute of Meteorological Research, Seogwipo, South Korea

Abstract Volcanic evolutions typically accompany significant changes in medium properties. Monitoring the seismic properties may be useful in identifying the state of volcanic evolution. Temporal variation of shallow crustal V_P/V_S ratios before and during the 2009 eruption of Redoubt Volcano, Alaska, is investigated using the *P* and *S* traveltimes of local earthquakes. High V_P/V_S ratios of ~1.9 are observed over a wide region in the precursory phase, suggesting the presence of partial melts in the medium at least several months before explosive eruptions. The high V_P/V_S ratios decrease until the early effusive phase with rates of -0.179 year^{-1} in the precursory phase (65 days) and -2.147 year^{-1} in the explosive phase (40 days), which is equivalent to a decrease in the bulk modulus of fluids by ~1.1 and 7.9 GPa, respectively. The decreasing V_P/V_S ratios in the precursory phase may be due to increasing amounts of overpressurized gas and water vapor in the medium. The rapid decrease in V_P/V_S ratios during the explosive phase may be caused by melt eruption and gas emission. The V_P/V_S ratios were observed to be nearly stationary since the early effusive phase, suggesting rare presence of melts and low levels of pore pressures with degassing. These observations suggest that monitoring V_P/V_S ratios may be useful to identify the eruption state.

1. Introduction

Timely notice of volcanic activity is crucial for the mitigation of imminent volcanic hazards. However, real-time inference of eruption status is difficult, and the temporal evolution of volcanic eruptions is poorly understood despite various efforts [*Huppert and Woods*, 2002; *Schmid et al.*, 2012]. Seismic properties (e.g., velocities and anisotropy) depend on the elastic modulus and the density of medium that change with the physical and chemical properties of the medium such as mineral (rock) composition, porosity, density, cracks (fractures), fluid saturation, temperature, and pressure [*Toksöz et al.*, 1976; *Ito et al.*, 1979; *Thurber et al.*, 1997; *Monna et al.*, 2003]. Thus, seismic analyses have been widely applied for the investigation of temporal medium property changes in active tectonic regions including earthquake rupture zones [*Hong and Menke*, 2006; *Yu and Hung*, 2012], geothermal regions [*Maeda et al.*, 2010], and active volcanic regions [*Brenguier et al.*, 2008; *Anggono et al.*, 2012]. In particular, the seismic velocity ratio, V_P/V_S, is readily convertible to the Poisson's ratio, which reflects the composition and physical properties of the medium [e.g., *Chatterjee et al.*, 1985]. The V_P/V_S ratios were found to be effective for monitoring volcanic regions [*Chiarabba and Moretti*, 2006; *Unglert et al.*, 2011; *Johnson and Poland*, 2013].

Redoubt Volcano is located in the northeastern Aleutian volcanic arc in the Cook Inlet, ~170 km southwest from Anchorage, Alaska (Figure 1). The volcano is a glaciated stratovolcano fed by rhyolitic andesitic magma [*Morrissey*, 1997]. Redoubt Volcano is 3108 m high, 10–12 km in diameter at the base, and ~1.5 km in diameter at the crater [*Bull et al.*, 2013]. The volcano erupted in 1902, 1933, 1966–1968, 1989–1990, and most recently in 2009 [*Coombs et al.*, 2013]. The precursory phase of the 2009 eruption began in July 2008, and explosive eruptions started on 15 March 2009. The effusive phase with lava dome growth began on 4 April 2009. The volcano stabilized since July 2009 (posteruption phase) [*Bull and Buurman*, 2013; *Grapenthin et al.*, 2013] (see supporting information).

2. Data

The Alaska Volcano Observatory (AVO) operated nine seismic stations around Redoubt Volcano at the time of the 2009 eruption (Figure 1). The spatial distribution of seismic stations displays good azimuthal coverage around the volcano. We analyze 4729 local earthquakes around Redoubt Volcano from January 2009 to December 2010. The events around the volcano display shallow seismicity (Figure 1). The event information,

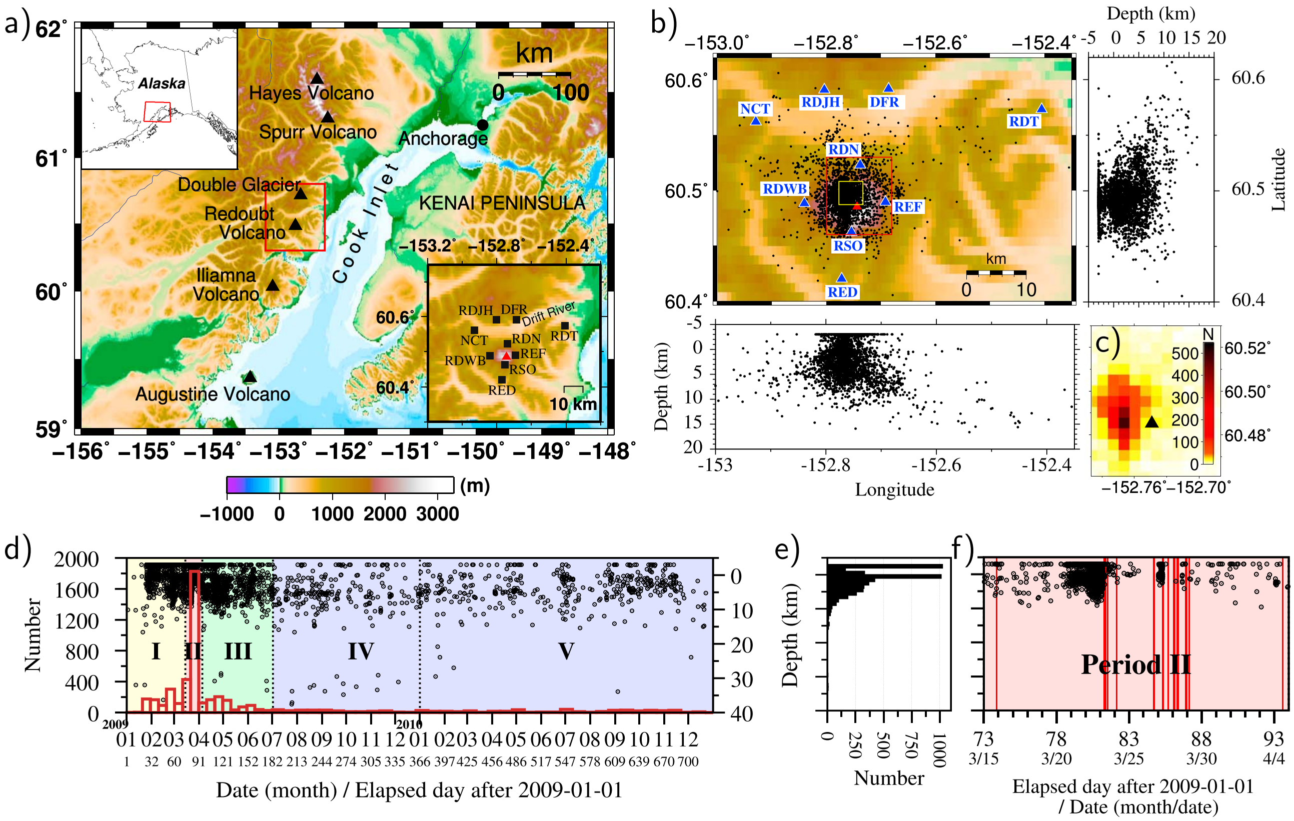

Figure 1. (a) Location of Redoubt Volcano. An inset of the enlarged map presents stations around the volcano. (b) Map view and cross-sectional views of seismicity (dots). (c) Seismicity density in the study region. (d) Event distribution (dots) with time and depth. The histogram in red presents the number of events for every 10 days. (e) A histogram of numbers of events with depth. (f) The dates of explosive eruptions (red lines) along with event distribution over time.

including P and S arrival times, was collected from the AVO seismic catalogs. The magnitudes (M_L) of events range between −0.9 and 3.5. Seismic records with epicentral distances less than 10 km and focal depths equal to or less than 10 km are analyzed.

The P and S arrival times are refined by manually reexamining the waveforms with high signal-to-noise ratios. The arrival times of waveforms with low signal-to-noise ratios are removed from the data set. We collect 3843 pairs of P and S traveltimes for 1936 local events. The traveltime data set is divided into five subsets based on the eruption phases and their durations (Figure 1; see supporting information). Period I comprises the precursory phase (1 January 2009 to 14 March 2009), period II is the explosive phase (15 March 2009 to 4 April 2009), period III is the effusive phase (5 April 2009 to 1 July 2009), and periods IV and V are the posteruption phase. Period IV lasts for 6 months after the effusive phase (2 July 2009 to 31 December 2009), and period V lasts for 1 year after period IV (1 January 2010 to 31 December 2010).

3. Methods and Process

The V_P/V_S ratio of the medium is calculated using a modified Wadati analysis that is based on the P and S traveltimes [*Yoshiyama*, 1957; *Jo and Hong*, 2013]:

$$\frac{V_P}{V_S} - 1 = \frac{(T_s - T_p)}{T_p}, \tag{1}$$

where T_P and T_S are the traveltimes of local P and S waves. The V_P/V_S ratio is determined from the slope of the least squares line for the traveltime data set. Here the implementation of differential traveltimes ($T_s - T_p$) allows us to identify the data with large errors in origin times and hypocenters. Traveltime data with deviations greater than 0.2 s from the least squares line are removed from the analysis (see supporting information). The determination of the least squares line and the removal of outliers are performed

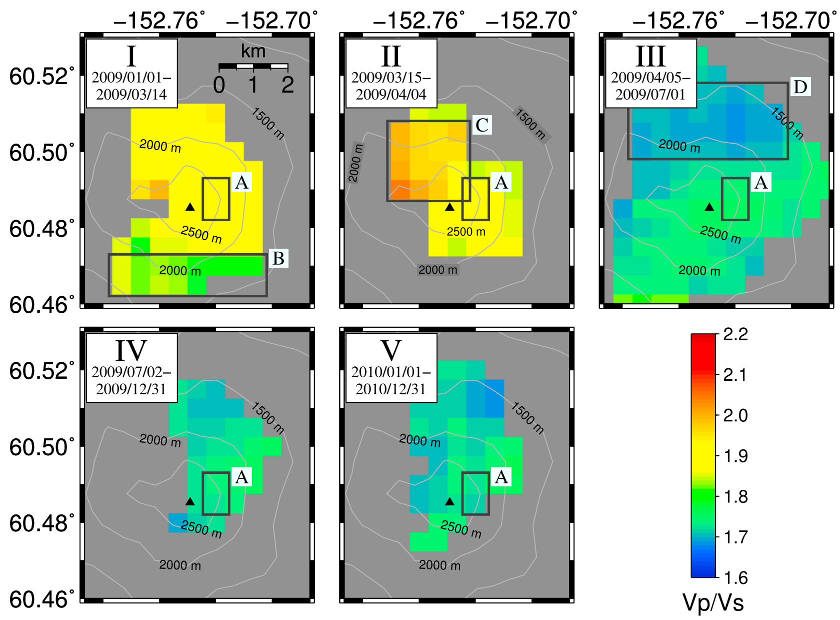

Figure 2. Spatial variations in V_P/V_S ratios by eruption phase from period I (precursory phase) to period V (posteruption phase). The V_P/V_S ratios are high in periods I and II and low in periods III to V. A central region around the summit (region A), unerupted southern region (region B), eruption site (region C), and posteruption northern region (region D) are marked.

iteratively until no further data are removed. The calculated V_P/V_S ratios can be translated directly into the Poisson's ratios, σ:

$$\sigma = \frac{1}{2}\left[1 - \frac{1}{(V_P/V_S)^2 - 1}\right]. \tag{2}$$

The dense monitoring system and high seismicity enable accurate estimation of V_P/V_S ratios for small and discretized regions. The study region is discretized by cells with a size of 0.04° in longitude and 0.02° in latitude. Cells overlap with adjacent cells by 0.03° in longitude and 0.015° in latitude so that the centers of the cells are placed every 0.01° in longitude and 0.005° in latitude. We collect the *P* and *S* traveltimes for event-station pairs of which central locations are placed in each cell. A representative V_P/V_S ratio is determined using the modified Wadati method for every cell with greater than 40 traveltime data (see supporting information). The depth of imaging is naturally constrained by the focal depths.

The V_P/V_S ratio can be expressed in terms of the effective bulk modulus, K_e, and effective shear modulus, μ_e:

$$\frac{V_P}{V_S} = \sqrt{\frac{K_e}{\mu_e} + \frac{4}{3}}. \tag{3}$$

For a porous medium, the effective bulk and shear moduli satisfy [*Gassmann*, 1951; *Husen et al.*, 2004]

$$\frac{K_e}{K_r - K_e} = \frac{K_d}{K_r - K_d} + \frac{K_f}{\phi(K_r - K_f)}, \quad \mu_e = \mu_d, \tag{4}$$

where K_r is the bulk modulus of the rock matrix, K_d is the bulk modulus of dry rock with empty pores, K_f is the bulk modulus of pore fluid, ϕ is the porosity of rock, and μ_d is the shear modulus of dry rock with empty pores. The temporal changes of V_P/V_S ratios can be attributed to variations in the bulk modulus of the fluid (see supporting information).

The stability of V_P/V_S estimates is tested using a bootstrapping resampling analysis [*Efron and Tibshirani*, 1991; *Hong and Menke*, 2008]. In addition, the effects of plausible errors in phase arrival and origin times on V_P/V_S estimates are quantified. These tests indicate that the results are stable and rarely dependent on the data sets selected and possible errors in the data sets (see supporting information).

10.1002/2014GL059408

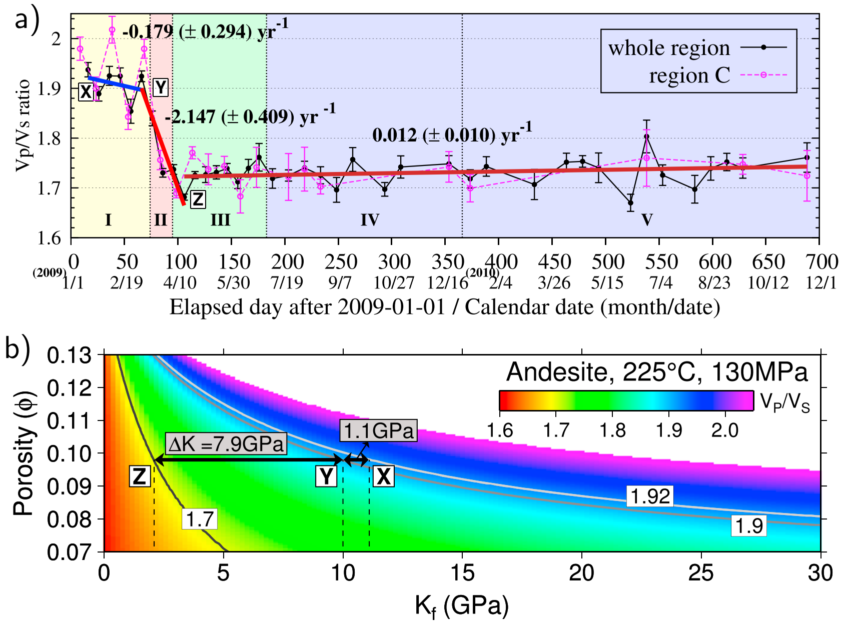

Figure 3. (a) Temporal variations in V_P/V_S ratios in the whole study region (black dots) and region C (purple dots). The least squares fitted lines for the whole-region data are presented with thick solid lines in blue (period I), red (period II), and brown (since early period III). The V_P/V_S ratios decrease consistently until early period III. (b) The changes in the bulk modulus of the fluid (K_f) equivalent to the decreases of V_P/V_S ratios during periods I and II for the porosity (ϕ) of 0.098. The decrease in V_P/V_S ratios during period I is equivalent to the apparent decrease in K_f by 1.1 GPa (X-Y) and that in period II to early period III by 7.9 GPa (Y-Z).

4. V_P/V_S Ratios as a Function of Eruption Phase

The V_P/V_S ratios of the shallow crust display characteristic variations with eruption phase (Figure 2). It is known that gas emission began with the melting of the summit glacier and the increases in temperature and seismicity during period I (precursory phase) [*Bull and Buurman*, 2013]. The V_P/V_S ratios for this phase are between 1.79 and 1.99, equivalent to the Poisson's ratios of 0.27–0.33 (see supporting information). The V_P/V_S ratios range between 1.85 and 2.05 (equivalently, Poisson's ratios of 0.29–0.34) during period II (explosive phase), in which intense explosive eruptions occurred. It is observed that the V_P/V_S ratios reach 1.90 in most regions. The high V_P/V_S ratios in the northwestern region during the explosive phase is consistent with those observed during the 1989–1990 explosions [*Benz et al.*, 1996]. The northwestern region illuminated by the peak V_P/V_S ratios agrees with the explosive eruption site.

The V_P/V_S ratios range between 1.69 and 1.83 (equivalently, Poisson's ratios of 0.23–0.29) during period III (effusive phase), in which explosive eruptions were completed when the crater is deflated and the lava domes began to grow. These V_P/V_S ratios are much lower than those of period II. Similar magnitudes of V_P/V_S ratios (1.68–1.76 and equivalently 0.23–0.26 in Poisson's ratios) are observed in periods IV and V (posteruption phase). The low V_P/V_S ratios in the effusive and posteruption phases may be associated with rare presence of fluids and a decrease in the pore pressure of the medium.

The average V_P/V_S ratios around the summit (region A) are 1.92 (±0.0032) in period I (precursory phase), 1.86 (±0.0004) in period II (explosive phase), 1.75 (±0.0053) in period III (effusive phase), and 1.73 (±0.0016) and 1.72 (±0.0051) in periods IV and V (posteruption phase). The high V_P/V_S ratios in the precursory phase suggest increases in temperature and cracks and the presence of melts in the medium [*Ito et al.*, 1979; *Tait et al.*, 1989; *Nakajima et al.*, 2001].

On the other hand, the southern region (region B) presents relatively low V_P/V_S ratios of 1.82 (±0.022) in period I, while the northern region displays high V_P/V_S ratios. In particular, the V_P/V_S ratios in the northwestern region (region C) are as high as 1.97 in period II. However, the V_P/V_S ratios in the northern region (region D) are as low as 1.69–1.71 in period III. The localized high V_P/V_S ratios around the northern region in period I implies that melts are fed from the northern region [e.g., *Nakajima et al.*, 2001]. It is observed that the V_P/V_S ratios return to their usual values after the completion of the explosive eruptions.

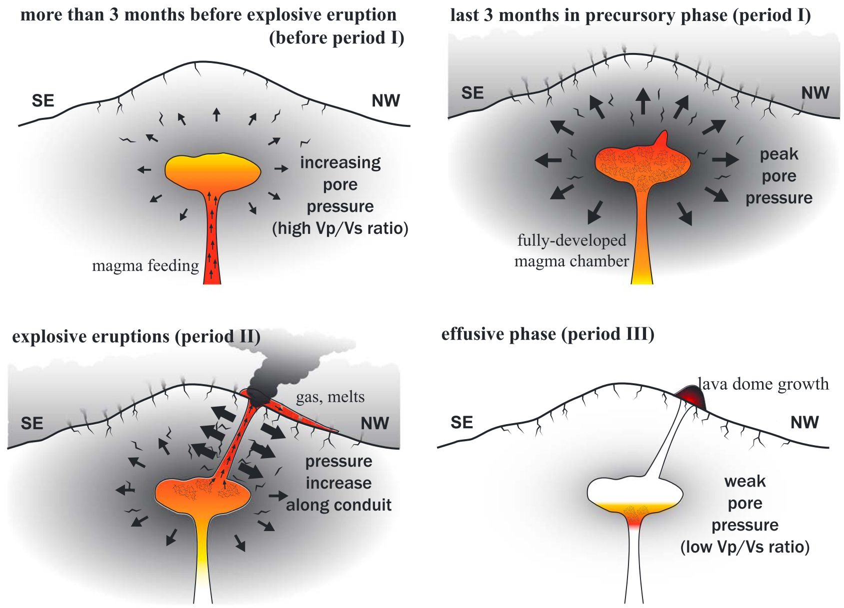

Figure 4. Schematic model of volcanic evolution over time. Redoubt Volcano was fully developed at least 3 months before the explosive eruptions began. Overpressurized gas and water vapor fill the pores in the medium around the summit in the early precursory phase and expand to a wide region with time. Explosive eruptions emit the melt and gas in the northwestern region, decreasing the pore pressure in the medium and developing cracks along the conduit. The pore pressure in the medium reaches its lowest level since the early effusive phase.

5. Temporal Variation of V_P/V_S Ratios

The temporal variations of V_P/V_S ratios are measured every 6–10 days during periods I to III and every 15 days during periods IV and V depending on the number of data available (Figure 3). The V_P/V_S ratios decrease continuously with time until early period III (effusive phase) over the whole region, which is observed also in the eruption site (region C). The V_P/V_S ratios are as high as ~1.90 on 21 March (period II) before 18 consecutive explosive eruptions and are slightly decreased to ~1.85 on 31 March 2009 after the consecutive explosive eruptions. The V_P/V_S ratios become ~1.73 on 10 April after completion of all explosive eruptions and decreased further to ~1.67 on 30 April. The temporal decay rate of V_P/V_S ratios during period II is much larger than that during period I, which is particularly strong in the eruption site (i.e., region C in Figure 2).

The temporal decay rate of V_P/V_S ratios for the 65 days between 1 January 2009 and 7 March 2009 (period I) is −0.179 (±0.294) year^{-1}, and that for the 40 days between 7 March and 16 April 2009 (period II) is −2.147 (±0.409) year^{-1}. On the other hand, the temporal decay rate of V_P/V_S ratios for the 625 days between 16 April 2009 and 31 December 2010 (since early period III) is 0.012 (±0.010) year^{-1}, indicating nearly stationary V_P/V_S ratios. The temporal decrease of V_P/V_S ratios in period I may be caused by increasing amounts of overpressurized gas and water vapor in the medium [e.g., *Chiarabba and Moretti*, 2006; *Unglert et al.*, 2011]. Significant amounts of melt and gas are erupted during period II, causing a steep decrease in V_P/V_S ratios.

The V_P/V_S ratio can be expressed in terms of effective bulk and shear moduli (K_e, μ_e), which are dependent on the porosity and composition of pore fluids (see supporting information). Here the bulk and shear moduli of the rock matrix (K_r, μ_r) are dependent on the chemical composition, temperature, and pressure. The temporal decay rates of the V_P/V_S ratios can be described as apparent decreases in the bulk modulus of the pore fluids [*Werner et al.*, 2013; *Yoshiyama*, 1957]. We calculate the bulk and shear moduli of andesite at a depth of 5 km from the bulk and shear moduli on the Earth's surface and their derivatives with respect to pressure and temperature. Here the temperature and lithostatic pressure at a depth of 5 km are set to be 225°C and 0.13 GPa, respectively [*Huppert and Woods*, 2002].

The high V_P/V_S ratios (~1.90) in the beginning of the explosive eruptions suggest that melts are present abundantly in the medium. The typical bulk modulus of melts (K_f) is ~10 GPa [*Gassmann*, 1951; *Jo and Hong*, 2013]. In this case, the porosity is determined to be 0.098 (Figure 3). When the porosity is assumed to be constant with time, the decrease in V_P/V_S ratio from 1.9 to 1.7 during the explosive eruptions (Y-Z in Figure 3) corresponds to an apparent decrease of K_f by 7.9 GPa. Similarly, the decrease in V_P/V_S ratio from 1.92 to 1.90 during the precursory phase (X-Y in Figure 3) corresponds to a decrease in K_f of 1.1 GPa.

6. Discussion and Conclusions

The V_P/V_S ratios decrease persistently in periods I and II. However, the decrease rates of V_P/V_S ratios during periods I (precursory phase) and II (explosive phase) are different due to differences in volcanic eruption states, fluid composition, and pressure. The V_P/V_S ratio of period I decreases due to an increase in overpressurized gas and water vapor in the medium, while that of period II decrease due to composite eruptions of melt and gas from the medium. The decrease rate of V_P/V_S ratio in period II (explosive phase) is larger than that in period I.

The peak V_P/V_S ratio occurring in the beginning of the precursory phase suggests that slowly ascending magma develops the magma chamber in the upper crust fully at least 3 months before the explosive eruptions (Figure 4). The fully developed magma chamber increases the amount of overpressurized gas in the medium with fractional degassing in the summit, causing a continuous decrease in V_P/V_S ratios [e.g., *Johnson and Poland*, 2013]. Furthermore, melts migrate from the magma chamber to the Earth's surface along the conduit during the several months prior to explosive eruptions, creating horizontal cracks and faults along the conduit during the last several months of the precursory phase [*Roman and Gardine*, 2013].

The explosive eruptions cause a significant reduction in melt content in the medium, accompanied by a rapid and consistent decrease in V_P/V_S ratio with time. Most melts were erupted by early period III (effusive phase), yielding low V_P/V_S ratios. The remaining gas leaks continuously from the medium during the effusive phase, yielding low V_P/V_S ratios. The low and stationary V_P/V_S ratios since early period III suggest no further active volcanic evolution. The apparent temporal variation of V_P/V_S ratios with volcanic evolution suggests that real-time monitoring of V_P/V_S ratios may be useful in identifying the volcanic eruption status.

Acknowledgments
We thank the Alaska Volcano Observatory (AVO) for making the seismic waveforms, source information, and initial phase arrival time information available. We are grateful to Sung Keun Lee from Seoul National University and Yongjae Lee from Yonsei University for valuable comments on the properties of volcanic medium. We thank the editor Andrew Newman and anonymous reviewers for valuable review comments that improved the paper. This work was supported by the Korea Meteorological Administration Research and Development Program under grant CATER 2012-8050.

The Editor thanks two anonymous reviewers for their assistance in evaluating this paper.

References

Anggono, T., T. Nishimura, H. Sato, H. Ueda, and M. Ukawa (2012), Spatio-temporal changes in seismic velocity associated with the 2000 activity of Miyakejima volcano as inferred from cross-correlation analyses of ambient noise, *J. Volcanol. Geotherm. Res.*, *247–248*, 93–107.

Benz, H. M., B. A. Chouet, P. B. Dawson, J. C. Lahr, R. A. Page, and J. A. Hole (1996), Three-dimensional *P* and *S* wave velocity structure of Redoubt Volcano, Alaska, *J. Geophys. Res.*, *101*(B4), 8111–8128.

Brenguier, F., N. M. Shapiro, M. Campillo, V. Ferrazzini, Z. Duputel, O. Coutant, and A. Nercessian (2008), Towards forecasting volcanic eruptions using seismic noise, *Nat. Geosci.*, *1*, 126–130.

Bull, K. F., S. W. Anderson, A. K. Diefenbach, R. L. Wessels, and S. M. Henton (2013), Emplacement of the final lava dome of the 2009 eruption of Redoubt Volcano, Alaska, *J. Volcanol. Geotherm. Res.*, *259*, 334–348.

Bull, K. F., and H. Buurman (2013), An overview of the 2009 eruption for Redoubt Volcano, Alaska, *J. Volcanol. Geotherm. Res.*, *259*, 2–15.

Chatterjee, S. N., A. M. Pitt, and H. M. Iyer (1985), Vp/Vs ratios in the Yellowstone National Park region, Wyoming, *J. Volcanol. Geotherm. Res.*, *26*, 213–230.

Chiarabba, C., and M. Moretti (2006), An insight into the unrest phenomena at the Campi Flegrei caldera from Vp and Vp/Vs tomography, *Terra Nova*, *18*(6), 373–379.

Coombs, M., T. Sisson, H. Bleick, S. Henton, C. Nye, A. Payne, C. Cameron, J. Larsen, K. Wallace, and K. F. Bull (2013), Andesites of the 2009 eruption of Redoubt Volcano, Alaska, *J. Volcanol. Geotherm. Res.*, *259*, 349–372.

Efron, B., and R. Tibshirani (1991), Statistical data analysis in the computer age, *Science*, *253*, 390–395.

Gassmann, F. (1951), Uber die Elastizitat poroser Medien, *Viertel. Naturforsch. Ges. Zürich*, *96*, 1–23.

Grapenthin, R., J. T. Freymueller, and A. M. Kaufman (2013), Geodetic observations during the 2009 eruption of Redoubt Volcano, Alaska, *J. Volcanol. Geotherm. Res.*, *259*, 115–132.

Hong, T.-K., and W. Menke (2006), Tomographic investigation of the wear along the San Jacinto fault, southern California, *Phys. Earth Planet. Inter.*, *155*, 236–248.

Hong, T.-K., and W. Menke (2008), Imaging laterally varying regional heterogeneities from seismic coda using a source-array analysis, *Phys. Earth Planet. Inter.*, *166*, 188–202.

Huppert, H. E., and A. W. Woods (2002), The role of volatiles in magma chamber dynamics, *Nature*, *420*, 493–495.

Husen, S., R. B. Smith, and G. P. Waite (2004), Evidence for gas and magmatic sources beneath the Yellowstone volcanic field from seismic tomographic imaging, *Phys. Earth Planet. Inter.*, *131*, 397–410.

Ito, H., J. DeVilbiss, and A. Nur (1979), Compressional shear waves in saturated rock during water-steam transition, *J. Geophys. Res.*, *84*, 4731–4735.

Jo, E., and T.-K. Hong (2013), V_P/V_S ratios in the upper crust of the southern Korean Peninsula and their correlations with seismic and geophysical properties, *J. Asian Earth Sci.*, *66*, 204–214.

Johnson, J. H., and M.-P. Poland (2013), Seismic detection of increased degassing before Kilauea's 2008 summit explosion, *Nat. Commun.*, *4*, 1668, doi:10.1038/ncomms2703.

Maeda, T., K. Obara, and Y. Yukutake (2010), Seismic velocity decrease and recovery related to earthquake swarms in a geothermal area, *Earth Planets Space*, *62*, 685–691.

Monna, S., L. Filippi, L. Beranzoli, and P. Favali (2003), Rock properties of the upper-crust in Central Apennines (Italy) derived from high-resolution 3-D tomography, *Geophys. Res. Lett.*, *30*(7), 1408, doi:10.1029/2002GL016780.

Morrissey, M. M. (1997), Long-period seismicity at Redoubt Volcano, Alaska, 1989–1990 related to magma degassing, *J. Volcanol. Geotherm. Res.*, *75*, 321–335.

Nakajima, J., T. Matsuzawa, A. Hasegawa, and D. Zhao (2001), Seismic imaging of arc magma and fluids under the central part of northeastern Japan, *Tectonophysics*, *341*, 1–17.

Roman, D. C., and M. D. Gardine (2013), Seismological evidence for long-term and rapidly accelerating magma pressurization preceding the 2009 eruption of Redoubt Volcano, Alaska, *Earth Planet. Sci. Lett.*, *371*, 226–234, doi:10.1016/j.epsl.2013.03.040.

Schmid, A., J. R. Grasso, D. Clarke, V. Ferrazzini, P. Bachèlery, and T. Staudacher (2012), Eruption forerunners from multiparameter monitoring and application for eruptions time predictability (Piton de la Fournaise), *J. Geophys. Res.*, *117*, B11203, doi:10.1029/2012JB009167.

Tait, S., C. Jaupart, and S. Vergnioille (1989), Pressure, gas content and eruption periodicity of a shallow, crystallising magma chamber, *Earth Planet. Sci. Lett.*, *92*, 107–123.

Thurber, C., S. Roecker, W. Ellsworth, Y. Chen, W. Lutter, and R. Sessions (1997), Two-dimensional seismic image of the San Andreas Fault in the Northern Gabilan Range, central California: Evidence for fluids in the fault zone, *Geophys. Res. Lett.*, *24*, 1591–1594.

Toksöz, M. N., C. H. Cheng, and T. Aytekin (1976), Velocities of seismic waves in porous rock, *Geophysics*, *41*, 621–645.

Unglert, K, M. K. Savage, N. Fournier, T. Ohkura, and Y. Abe (2011), Shear-wave splitting, Vp/Vs, and GPS during a time of enhanced activity at Aso caldera, Kyushu, *J. Geophys. Res.*, *116*, B11203, doi:10.1029/2011JB008520.

Werner, C., P. J. Peter, M. Doukas, T. Lopez, M. Pfeffer, R. BcGimsey, and C. Neal (2013), Degassing of CO_2, SO_2, and H_2S associated with the 2009 eruption of Redoubt volcano, Alaska, *J. Volcanol. Geotherm. Res.*, *259*, 270–284.

Yoshiyama, R. (1957), The ratio of the velocity of P and S waves, *Bull. Earthq. Res. Inst.*, *35*(4), 627–640.

Yu, T.-C., and S.-H. Hung (2012), Temporal changes of seismic velocity associated with the 2006 Mw 6.1 Taitung earthquake in an arc-continent collision suture zone, *Geophys. Res. Lett.*, *39*, L12307, doi:10.1029/2012GL051970.

